AD_____

Award Number: DAMD17-97-1-7116

TITLE: Contrast Enhanced 3D Color Amplitude Imaging of the Breasts

PRINCIPAL INVESTIGATOR: Flemming Forsberg, Ph.D.

CONTRACTING ORGANIZATION: Thomas Jefferson University
Philadelphia, Pennsylvania 19107

REPORT DATE: October 2001

TYPE OF REPORT: Final

PREPARED FOR: U.S. Army Medical Research and Materiel Command
Fort Detrick, Maryland 21702-5012

REPORT DOCUMENTATION PAGE

Form Approved
OMB No. 074-0188

1. AGENCY USE ONLY (Leave blank)	2. REPORT DATE	3. REPORT TYPE AND DATES COVERED
	October 2001	Final (15 Sep 97 - 14 Sep 01)

4. TITLE AND SUBTITLE
Contrast Enhanced 3D Color Amplitude Imaging of the Breasts

5. FUNDING NUMBERS
DAMD17-97-1-7116

6. AUTHOR(S)
Flemming Forsberg, Ph.D.

7. PERFORMING ORGANIZATION NAME(S) AND ADDRESS(ES)
Thomas Jefferson University
Philadelphia, Pennsylvania 19107

E-Mail: forsberg@esther.rad.tju.edu

8. PERFORMING ORGANIZATION REPORT NUMBER

9. SPONSORING / MONITORING AGENCY NAME(S) AND ADDRESS(ES)
U.S. Army Medical Research and Materiel Command
Fort Detrick, Maryland 21702-5012

10. SPONSORING / MONITORING AGENCY REPORT NUMBER

11. SUPPLEMENTARY NOTES
Report contains color

12a. DISTRIBUTION / AVAILABILITY STATEMENT
Approved for Public Release; Distribution Unlimited

12b. DISTRIBUTION CODE

13. ABSTRACT *(Maximum 200 Words)*
In total, 55 patients with 16 cancers and 39 benign lesions were enrolled in the study, which was less than anticipated. Standard 2D ultrasound achieved a sensitivity of 73% and a specificity of 58%, while 3D produced 75% and 36%, respectively. Contrast increased 3D sensitivity to 88% and specificity to 47%. The area under the ROC curve for the detection of breast cancer was 0.55 for 2D contrast, 0.60 for 3D ultrasound and 0.76 for 3D CAI with contrast ($p<0.03$). Mammography produced an area of 0.86, which was significantly higher than all ultrasound modalities ($p<0.025$) except 3D contrast ($p=0.16$). When mammography was combined with 2D contrast the area increased to 0.88, with 3D contrast to 0.89, and with all ultrasound modalities to 0.96 ($p<0.001$). The vascularity and the presence of anastamoses observed with 3D contrast were the only significant markers of malignancy found ($p<0.02$). In a subset of 17 patients, 2D contrast provided some quantitative parameters, which correlated with direct pathologic vascularity assessments such as the iMVD. Specifically, the microvessel area and density for vessels 30 to 39 μm in diameter were most significant. Overall these results validate the fundamental hypothesis of this project; namely that the combination of 3D CAI and an ultrasound contrast agent increases the ability to diagnose breast cancer relative to current techniques.

14. SUBJECT TERMS	15. NUMBER OF PAGES
Breast Cancer, 3D ultrasound imaging, ultrasound contrast agent	40
	16. PRICE CODE

17. SECURITY CLASSIFICATION OF REPORT	18. SECURITY CLASSIFICATION OF THIS PAGE	19. SECURITY CLASSIFICATION OF ABSTRACT	20. LIMITATION OF ABSTRACT
Unclassified	Unclassified	Unclassified	Unlimited

3. TABLE OF CONTENTS

1. FRONT COVER.....1

2. SF 298.....2

3. TABLE OF CONTENTS.....3

4. INTRODUCTION.....4

5. BODY.....5

5.1 Methods 5

5.2 Results and Discussion 7

6. KEY RESEARCH ACCOMPLISHMENTS.....12

7. REPORTABLE OUTCOMES.....12

8. CONCLUSIONS.....14

9. REFERENCES.....16

10. TABLES.....18

11. FIGURES.....22

12. APPENDICES.....26

4. INTRODUCTION

The goal of any breast imaging modality is to improve the early detection of tumors and to improve the differentiation between benign and malignant lesions. While x-ray mammography is efficacious in diagnosing a high percentage of breast masses, it also produces a high rate of false positives [1]. The percentage of breast biopsies that are actually malignant vary between 10 % and 35 %. Thus, a technique which reliably differentiates between malignant and benign masses would improve the diagnosis of breast cancer and should, therefore, reduce the number of negative biopsies as well as the trauma of the patients. This project attempts to establish such a technique through the novel and innovative combination of three-dimensional (3D) ultrasound imaging with a contrast agent.

Ultrasound imaging is currently an auxiliary modality in breast imaging. It is mainly used to differentiate between cystic and solid lesions [2]. Investigations into the possibility of breast cancer diagnosis based on Doppler ultrasound flow detection have produced mixed results, due to overlap between flow measurements in benign and malignant tumors [3-4]. One problem may be the lack of sensitivity in flow detection in small tumor vessels using ultrasound. This hypothesis is supported by reports in the pathology literature describing angiogenic vascular morphology as an independent predictor of metastatic disease [5].

Ultrasound contrast agents produce increases of 15 to 25 dB in the echo intensities of blood flow signals; especially when combined with a new display technique called color amplitude imaging (CAI) [6-7]. Thus, an interesting research study can be devised, which compare the ability of two-dimensional (2D) color Doppler ultrasound with and without contrast to differentiate between benign and malignant masses relative to x-ray mammography. This is in essence the purpose of a 5 year National Institutes of Health (NIH) funded project recently awarded to Thomas Jefferson University. The current project (DAMD17-97-1-7116) is an expansion to the NIH project which adds 3D flow imaging with and without contrast, since 3D imaging should be better suited than 2D ultrasound to demonstrate the tortuous angiogenic vasculature associated with breast cancer.

Not only is the potential of the novel combination of 3D imaging and contrast in itself innovative, but because of the NIH funded study it will be possible to compare a number of new and unique approaches to breast cancer diagnosis i.e., 2D and 3D CAI with and without contrast as well as harmonic imaging directly to x-ray mammography. Furthermore, this project is extremely cost-effective because the NIH grant coves a majority of the personnel costs as well as all major equipment purchases. The amalgamation of the NIH project with the current proposal also allows for basic research into the correlation between Doppler flow signals and pathologically detected lesion vascularity. This will enable a deeper understanding of the relationship between tumor neovascularity and ultrasound flow measurements; again at very little cost to this proposal.

Consequently, this project is an add-on study to the already funded NIH project aimed at increasing the sensitivity and specificity of breast ultrasound by combining injection of an ultrasound contrast agent with 3D reconstruction of color amplitude images. The fundamental

hypothesis is that the neovasculature of malignant lesions can be visualized with this novel combination, thus, improving the diagnosis of breast cancer.

5. BODY

The central hypothesis of this project is that the differentiation between benign and malignant breast lesions can be improved by visualization of tumor neovascularity using 3D ultrasound imaging in conjunction with an ultrasound contrast agent. To investigate this hypothesis 150 women with breast lesions will be recruited over three years and imaged using contrast enhanced 3D CAI. The specific tasks of the project (as presented in the original Statement of Work) can be found in Appendix I.

First, an outline of the methods applied will be given followed by a presentation of the results to date. Finally, the conclusions and future directions of the research will be discussed.

5.1 Methods

The 3D CAI reconstructions in this project were performed with a state-of-the-art ultrasound scanner connected to an LIS 6000A 3D Image Acquisition and Reconstruction system (Life Imaging Systems Inc, London, Canada). All 3D CAI acquisitions were performed with an HDI 3000 scanner (Advanced Technology Laboratories, Bothell, WA). The 3D CAI data sets were reconstructed, with no loss of registration accuracy, to provide both multi-perspective Maximum-Intensity-Projection visualization and 2D planar views.

The patients used in this project were women of a wide variety of ages having a breast mass or abnormality resulting in a breast excisional biopsy. Breast cancer in males accounts for only about 1 % of cases in our hospital and thus, were not be included in the patient population. All patients were referred after X-ray mammography identified a mass or suspicious area. The target enrollment was approximately 50 patients per year, which represented half of the patients being recruited for the NIH-supported study.

Following a baseline ultrasound grayscale scan, which identified the mass seen by x-ray mammography, images for 3D CAI of the lesion were acquired. Next, an ultrasound contrast agent was administered intravenously via a peripheral vein, preferably the antecubital vein. The agent used was either Levovist injection (Berlex Laboratories, Montville, NJ) or Optison (Mallinckrodt, St. Louis, MO) in 10 ml and 1.0 ml dosages, respectively. An initial videotaped sweep of the mass was made with the gain and CAI settings unaltered from the pre contrast settings. This allowed for side by side comparison of pre and post contrast CAI studies. Following this, the CAI settings were optimized for the stronger contrast enhanced Doppler signals. As the SNR improves it was possible to achieve higher frame rates and/or line density, improving spatial resolution of the color. Videotaped sweeps of the abnormality were made every 1 to 2 minutes through the period of enhancement (up to 6 minutes). A second injection was made to acquire 3D CAI data with the gain and other settings unaltered from the pre contrast protocol. This allowed for side by side comparison of pre and post contrast 3D CAI studies.

Next the CAI settings were optimized for the stronger contrast enhanced signal, and 3D data acquired again.

Each mammogram was read by one radiologist. Evaluation of the ultrasound studies were performed by one of two radiologists. The pre- and post-contrast 2D and 3D ultrasound diagnoses were made on a six-point scale: 0) no lesion seen (no findings), 1) benign, 2) probably benign, 3) indeterminate, 4) probably malignant, and 5) malignant. The 2D and 3D readings were performed at least 3 months apart to eliminate any bias. Each radiologist evaluated pre- and subsequently post-contrast diagnostic ultrasound criteria.

All imaging variables collected were compared to all histopathological variables. The pre- and post-contrast 2D and 3D ultrasound diagnostic criteria included: overall diagnosis; the size, shape, and orientation of the lesion; echogenicity compared to surrounding tissue; degree of enhancement (none, mild, good, excellent and excessive); tumor margin definition; through transmission characteristics; degree of vascularity; blood vessel characteristics; vessel anastamoses; and pattern of vascularity. The histopathological variables included: diagnosis; estrogen and progesterone receptor presence or absences; k167 and p53 marker percentages; presence or absence of hemorrhagic, necrotic, or other component of the lesion; location of hemorrhagic, necrotic, or other component in the lesion; histological margins; TNM staging; histological lesion type; presence or absence of vascular invasion; histological and cytological grade; presence or absence of metastases; node staging; and percentage of the lesion that was invasive or in situ.

In a subgroup of patients, the ultrasound findings were further correlated to the pathology sections. After removal of the mass, the specimens were sectioned in the same plane as the ultrasound images and stained with an endothelial cell marker, CD31, which targets the microvessel walls staining them brown to dark brown in color. Finally, the sections were mounted onto 2"x 3" glass slides. The vascular morphology of the tissue, specifically, the number and area occupied by tumor vessels, were determined by a semi-automated histomorphometry system based on SMZ-10A microscope (Nikon, Melville, NJ) and ImagePro Plus software (Media Cybernetics, Silver Spring, MD). Using the software, microscope, and a Sony CCD camera, the entire specimen area was captured and digitized under 100x magnification. The frame size captured is equal to 640 pixels by 480 pixels or 1.27 mm^2. The number of color pixels on the color flow images relative to the pixel size of the mass was used as a first order measure of mass vascularity [8]. Frozen ultrasound images were captured before and after contrast injection and digitized using the image analysis software.

Both the slide and video image analyses are patterned after chromaticity analysis methods as described below (and originally in the Annual Report for Year 1). For each slide the total microvessel area (MVA) and count (MVC) were determined and divided into five categories: vessel diameters between a) 10-19 μm, b) 20-29 μm, c) 30-39 μm, d) 40-49 μm, and e) 50 μm and above. The ultrasonic image processing consisted of extracting red, green, and blue images and performing mathematical morphometry to obtain an image only with color pixels. From the video analysis, the percent of color pixels within the mass was calculated for each level before and after contrast administration.

Statistical Analysis

Primary comparisons of sensitivities and specificities for detecting cancer with different imaging modalities against the histopathological gold standard were conducted with McNemar's Q. Incremental validity of imaging diagnosis and mammography was analyzed using logistic regression and receiver operating characteristics (ROC) analyses. The small sample size led to a focus on bivariate analyses rather than the more complicated multivariate methods. All histopathological variables were compared with imaging judgements on diagnoses and characteristics of vascularity for the different modalities. When both sets of variables were nominal, chi-square tests were conducted. When both types of variables were ordinal or continuous, correlations were calculated. When one type of variable was nominal and one continuous non-parametric rank order tests such as Mann-Whitney U-tests or Kruskal-Wallis tests were performed.

To determine if a linear relationship existed between pathologic and ultrasonic vascularity measurements, an equal number of data points must be assessed from both methods. Ten ultrasonic data points per patient (5 pre and 5 post contrast) were consistently obtained because a hand held transducer was used and regardless of the size of the mass, scans at five levels of each mass can always be taken (albeit, sometimes with overlap between the levels). However, due to the size of some masses, five pathologic sections of a mass were sometimes not possible. Therefore, to be able to compare the data sets two solutions were developed, which ensured equal number of points in both data sets. One solution required ultrasonic data to be averaged and replaced until for each patient the number of scans equals the number of pathology slides (i.e., data reduction). The other solution required pathologic data to be averaged and added to the number of slides for each patient until five data points were reached (i.e., data expansion). The linear relationship between ultrasonic and pathologic data was assessed using single and multiple variable linear regression techniques.

5.2 Results and Discussion

Patient recruitment and data collection was scheduled to start in month 1. However, Life Imaging Sciences experienced some logistical problems and it took 3 months to get a LIS 6000A color system to Thomas Jefferson University. Following system calibration patient recruitment commenced in January 1998. Between January 1998 and January 1999, 22 patients (with 6 cancers and 16 benign lesions) were enrolled in the project and studied using contrast enhanced 3D CAI with Levovist. These numbers were less than anticipated, due mainly to difficulties in enrolling patients into a 4 hour ultrasound contrast agent study immediately prior to their breast surgery.

Moreover, there was one adverse event following a Levovist contrast study on April 7th 1998 where a patient experienced upper arm pain (reported in the Annual Report for Year 1). The patient was hospitalized on April 17th and discharged on the 18th. The event was upgraded from a mild to a serious adverse event on April 22nd, 1998 (due to the hospital admission). That day Cathy Smith of the US Army Medical Research and Material Command was notified by phone and a written report was sent on April 23rd, 1998. This adverse event was classified as a rated side effect of Levovist and no changes to the study protocol was, therefore, instigated.

More importantly, an interim data analysis of the 22 patients enrolled in this study, as envisaged under task 3, as well as of all the 79 patients recruited in the NIH funded study was completed and it indicated that Levovist was not as efficacious as expected [9]. Consequently, it was decided to change the ultrasound contrast agent to Optison (as described in the Annual Report for Year 2) which is a third generation agent (unlike Levovist) and is approved by the FDA for use in echocardiography. Optison was well tolerated by patients and safety issues related to the agent were not a concern in this study. However, this decision led to a four month stop in patient recruitment, while the associated protocol changes were implemented. As an added benefit the examination time was reduced from 4 hours to 1 hour, since less safety data was required for a contrast agent already approved for another indication. From May of 1999 and until the end of the study 33 patients with 11 cancers and 22 benign lesions were enrolled in the Optison arm of the study (this period included one year without a research coordinator, during which time no patients were recruited; as detailed in the Annual Report of Year 3).

Thus, the total patient population available from this study was 55 cases. The patients were predominantly Caucasian (41 women or 75 %), 13 (24 %) were African-American and one patient requested to be listed as "other". There were as mentioned 17 cancers and 38 benign lesions in this study. The mean age was 52 years. There were no statistical differences in neither age nor lesion size between benign and malignant cases (Table 1). Mammography findings were available for 50 subjects, biopsy for 54, while 2D and 3D ultrasound (with and without contrast) were obtained in 53 and 52 cases, respectively. Of the 50 patients who had all four measures, 15 (30%) had malignant breast lesions. Examples of 2D as well as 3D ultrasound imaging of breast lesions are presented in Figures 1 and 2.

Although the initial grant proposal anticipated a subject population of 150 patients, only 55 patients were enrolled in the study. There were approximately 300 patients screened for enrollment into the study per year with an average of 20 enrolled. The low recruitment rate was influenced by several factors. First, the contrast agent initially used for the study, Levovist, had not yet received FDA approval and was considered to be in the Phase II investigational phase, requiring extensive safety data records. This resulted in the procedure lasting approximately four hours. Because most women at Thomas Jefferson University Hospital are scheduled for breast surgery with one weeks notice, many working women could not accommodate the time-consuming study. Second, many subjects were uncertain about participating in a trial with an unapproved agent. When utilizing an FDA approved contrast agent (Optison), which reduced the procedure time to one hour, enrollment did increase; albeit not as much as hoped for. We found that the added pressure of participating in a trial, which would be of no direct benefit to the patient, was too much for many women to handle.

Among the 55 subjects standard 2D CAI achieved a sensitivity of 73 % and a specificity of 58 %, while 3D imaging produced 75 % and 36 %, respectively (Table 2). Contrast increased 3D sensitivity to 88 % and specificity to 47 %, while mammography achieved a sensitivity of 100 % and a specificity of 41 %. There were no statistically significant differences in specificity. The sensitivity of mammography exceeded all ultrasound modalities ($p < 0.01$). The sensitivity of 3D ultrasound was significantly higher than that of 2D ultrasound ($p = 0.046$). Furthermore, 3D with contrast did better than both baseline 3D and 2D ultrasound ($p = 0.008$ and $p = 0.018$, respectively) and better than grayscale ultrasound ($p = 0.039$).

The area under the ROC curve (A_z) for the detection of breast cancer was significantly higher for contrast enhanced 3D CAI (0.76) than for 2D with and without contrast (0.55 and 0.66, respectively) as well as for 3D ultrasound without contrast (A_z = 0.60; $p < 0.03$; Table 3). Mammography produced an area of 0.86, which was significantly higher than that of all the ultrasound modalities ($p < 0.025$) except 3D ultrasound with contrast ($p = 0.16$). The individual ROC curves obtained in this project are shown in Figure 3. These results validate the fundamental hypothesis of this project; namely that the combination of 3D CAI and an ultrasound contrast agent increases the ability to diagnose breast cancer over and above the current ultrasound modes (and en par with mammography).

Somewhat surprisingly, the A_z of 2D ultrasound was significantly higher without than with contrast ($p = 0.026$). This is contrary to the results of the NIH funded study (using only Levovist) where contrast enhanced 2D CAI achieved an A_z statistically no different from 2D without contrast [9]. The different results are most likely due to the small sample sizes (79 versus 55 subjects), which indicates that care must be taken when interpreting/extrapolating the results of the current study to the general population.

Logistical regression techniques were used to combine mammography with each of the 5 ultrasound imaging modes and to repeat the ROC analysis. This produced A_z's of 0.88 and 0.89 (Table 4), which were not statistically different from mammography alone. More encouraging the combination of all 5 ultrasound modes (i.e., without considering mammography) resulted in an A_z of 0.83; again not statistically different from mammography. Finally, mammography combined with all ultrasound modalities produced an A_z of 0.96, which was significantly higher than all other combinations and mammography alone ($p < 0.05$). The only exception was the combination of mammography and 3D baseline, which showed a trend towards significance ($p = 0.068$). Selected examples (since most are very similar) of the combined ROC curves are presented in Figure 4.

All the results reported above have assumed that the two contrast agents were sufficiently similar to allow the data to be analyzed as a whole. This assumption was tested by calculating sensitivity and specificity as well as the ROC curves split by agent (Table 5). There were no statistically significant differences in specificity for the two agents. When comparing the sensitivity of 2D and 3D imaging with Optison (50 % and 91 %) to 2D and 3D CAI with Levovist (60 % and 80 %) only the latter was significantly higher ($p = 0.007$). Moreover, in all cases the ROC analysis demonstrated no statistically significant differences due to agent. Hence, we continued to analyze the data set independent of which contrast agent was used.

Most of the comparisons between the ultrasound imaging results and the histopathological variables were not significant. However, the presence or absence of anastamoses assessed with contrast enhanced 3D CAI correlated significantly with the pathological diagnosis of benign/malignant breast tumors ($p = 0.007$). This indicates that the chaotic morphology of tumor neovascularity can indeed be evaluated with 3D contrast as hypothesized in the original grant application. Moreover, linear regression showed that contrast enhanced 2D and 3D assessments of anastamoses correlated ($r^2 = 0.47$; $p = 0.002$), which suggests that the added dimensionality of 3D imaging is an important factor. The pathologists diagnosis of

benign/malignant also correlated with the degree of vascularity seen in 3D contrast imaging ($p = 0.02$) showing the synergistic effect of combining 3D CAI with an ultrasound contrast agent. Especially, since the degree of vascularity of 2D and 3D contrast correlated ($r^2 = 0.44$; $p = 0.003$), but only the latter was a marker for malignancy.

The enhancement produced in 2D and 3D mode was assessed on a five point scale (none, mild, good, excellent and excessive). The chi-square analysis revealed that 3D contrast signals were more likely to be deemed acceptable (i.e., mild to excellent enhancement) than 2D contrast signals ($p = 0.01$). Finally, the degree of enhancement in 3D CAI mode correlated with tumor staging (i.e., stage 0, 1, 2, 3 or 4) with an r^2 value of 0.67 ($p = 0.012$). However, there were only 13 observations in this very small data set, which may influence the importance attached to this result.

The first task for the histomorphometry system was to develop image analysis software to allow a computerized histogram of the distribution of vessels and the number of vessels within the tumor to be produced from the pathology slides. The aim of the slide image analysis is to develop a method in which only microvessels with lumen would be recognized by the software and, hence, counted and measured. Only vessels with lumen will be chosen for three reasons: 1) the diameter of the vessels can be assessed directly, 2) other structures sporadically stained will not give false positives, and 3) a more repeatable and automated method can be performed. RGB color space poorly disperses the various color values and hence for biological images, where colored stains are commonly used to identify features, it is difficult to interpret the meanings of the separate RGB color channels. Therefore, the RGB images were converted to Hue Saturation Intensity (HSI) images, which do separate different regions of color values. HSI color space is closely related to the concepts of tint, shade, and tone and the meanings of HSI color channels for stained biological images can be stated as follows:

1) The hue channel identifies where a particular stain is located
2) The saturation channel corresponds to the amount of the stain
3) The intensity channel indicates the overall density of the stain.

The method used in this analysis was patterned after the chromaticity or color based analysis method used by Barbareschi et al. and Bell et al., respectively [10-11]. Additional processing techniques were applied due to the varying intensity of immunostaining and the use of a lower magnification power on the microscope. The method is described step by step in Table 6.

The measurements quantified by the software were the area, average diameter, and minimum diameter of each vessel. The average diameter is determined by the software as the average length of the diameters measured at 2 degrees of intervals and passing through the object's centroid. The minimum diameter is the length of the shortest line joining two points of the object's outline and must pass through the centroid. Depending on vessel orientation and cutting angle of the mass, the vessel diameter could be erroneously measured. If the vessel was parallel to the cutting angle then a larger diameter could result than if the vessel was oriented perpendicular to the cutting angle. To limit this particular error, the actual diameter of a vessel was determined by comparing the minimum and average diameter. If the average diameter was 3 times greater than the minimum diameter then it was assumed that the vessel appeared longitudinally and the minimum diameter was used as the vessels actual diameter. Otherwise, the average diameter was accepted as the vessels actual diameter. The number of vessels and

percent of area the vessels occupied were the results obtained and were divided into five categories as mentioned previously.

A subset of 17 patients (11 benign and 6 malignant masses) with 52 pathology slides (for a total of 8026 frames) were examined with the histomorphometry system. A total of 170 digitized ultrasound scans (5 pre and 5 post contrast for each patient) were included in this part of the study. There was a significant increase in the number of ultrasound color pixels pre to post contrast injection ($p < 0.02$). No statistical difference in ultrasonic color pixels was found between the benign and malignant masses. Table 7 gives the r^2 values for the linear regression for the reduced and expanded data sets. The multiple linear regression technique for the entire data set (i.e., benign and malignant lesions evaluated jointly) found significant correlations for ultrasonic color pixels post injection with the percent of area in the five vessel ranges (expanded MVA: $p = 0.0002$; reduced MVA: $p = 0.04$) and with the percent of vessels in the five vessel ranges ($p = 0.003$ and < 0.0001; expanded and reduced iMVD, respectively). No correlations were found between pre contrast ultrasonic color pixels and pathologic vascularity measurements using the entire data set.

When the data was analyzed separately for benign and malignant cases, some statistically significant correlations were found between pre contrast ultrasound and, in particular, malignant pathological variables (Table 7). However, as the number of cases is quite small (6 cancers only) it would be premature to attach too much importance to these results.

To determine which variable in the multiple linear regression contributed the most, the T-statistic was evaluated for each variable. The significant T-values are listed for the reduced and expanded data sets in Tables 8 and 9, respectively. For both the percent of area and percent of vessels in the five vessel ranges, the 30 to 39 μm vessel range contributed the most significantly to the linear relationship with the percent of color pixels post contrast injection, ($p < 0.0001$ expanded as well as $p = 0.002$ and $p < 0.0001$ reduced data).

From the statistical analysis, it can be inferred that contrast enhanced color flow imaging provides some quantitative parameters, which correlate with direct pathologic vascularity assessments such as the iMVD. Specifically, the microvessel area and count for vessels 30 to 39 μm in diameter were most significant. This is in agreement with the qualitative observations of Burns et al. [12]. These results indicate that ultrasound imaging with contrast may produce a quantitative measure of the neovascularity within breast tumors; similar to results recently obtained with MRI [13]. However, the current patient population in the sub-study is somewhat small and further cases are currently being analyzed.

The quantitative sub-study correlating contrast enhanced ultrasound and pathology has been presented at the AIUM and the Era of Hope, DoD Breast Cancer Research Meeting [14-15]. Overall results have also been published in a peer-reviewed journal [16-17]. Moreover, the main results of this project have been submitted to the AIUM annual conference in 2002 [18-19]. Finally, we expect to submit two manuscripts to peer-reviewed journals (most likely Radiology and Journal of Ultrasound in Medicine) describing the ROC analysis and the pathology sub-study, respectively.

6. KEY RESEARCH ACCOMPLISHMENTS

- In total 55 patients studied using contrast enhanced 3D CAI.
- The area under the ROC curve for the detection of breast cancer was significantly higher for 3D contrast (0.76) than for 2D with and without contrast and for 3D ultrasound without contrast ($p < 0.03$).
- Mammography produced an area under the ROC curve of 0.86, which was significantly higher than all ultrasound modalities ($p < 0.025$) EXCEPT 3D ultrasound with contrast ($p = 0.16$).
- Mammography when combined with all ultrasound modalities produced an area under the ROC curve of 0.96, which was a statistically significantly increase compared to mammography alone ($p = 0.01$).
- There were no significant differences between the performance of the two contrast agents except that the sensitivity of 3D imaging was higher with Optison than with Levovist ($p = 0.007$).
- The vascularity and the presence of anastamoses observed with contrast enhanced 3D were the only significant markers of malignancy found ($p < 0.02$).
- Marked increase in vascularity seen pre to post contrast imaging ($p < 0.02$).
- Contrast enhanced color flow imaging provides some quantitative parameters, which correlate with direct pathologic vascularity assessments ($p \leq 0.04$).
- Contrast enhanced ultrasound images of breast tumor vascularity correspond mainly to vessels 30 to 39 μm in diameter ($p = 0.002$ and $p < 0.0001$).

7. REPORTABLE OUTCOMES

Manuscripts, abstracts, presentations

Forsberg F, Goldberg BB: Contrast-enhanced ultrasound imaging. *Science & Medicine*, 5: 54 - 63, 1998.

Chaudhari MH, Forsberg F, Voodarla A, Saikali FN, Goonewardene S, Needleman L, Shi WT, Finkel GC, Goldberg BB: Breast tumor vascularity identified by contrast enhanced ultrasound and pathology: initial results. *Ultrasonics*, 38, 105 – 109, 2000.

Forsberg F, Rawool NM, Merton DA, Liu JB, Goldberg BB: Contrast enhanced vascular 3D ultrasound imaging. Accepted for publication in *Ultrasonics,* 2002.

Forsberg F, Chaudhari MH, Voodarla A, Goonewardene S, Needleman L, Goldberg BB: Quantifying breast tumor neovascularity by contrast enhanced ultrasound and pathology: a comparative study. *J Ultrasound Med*, 19, S56 – S57, 2000.

Forsberg F, Chaudhari MH, Merritt CRB, Needleman L, Maitino AJ, Voodarla A, Goonewardene S, Goldberg BB. Contrast enhanced ultrasound imaging of breast tumors. *Proc Era of Hope, DoD Breast Cancer Research Meet*, 257 – 258, 2000.

Forsberg F, Shi WT, Merritt CRB, Solcova M, Dai Q, Goldberg BB. Does the Mechanical Index Predict Destruction Rates for Contrast Microbubbles ? *J. Ultrasound Med*, vol. 20, pp. S12 – S13, 2001.

Goldberg BB, Merritt CRB, Needleman L, Piccoli CW, Forsberg F, Parker L, Maitino A, Merton DA, Schultz SM, Rawool NM. Contrast Enhanced Ultrasound and Mammography for Breast Cancer Detection. *J Ultrasound Med*, 20: S95, 2001.

Forsberg F, Shi WT, Merritt CRB, Dai Q, Merton DA, Huang MW, Solcova M, Goldberg BB. In Vitro and In Vivo Destruction of US Contrast Microbubbles is Independent of the Mechanical Index. *Radiology*, 2001. In press.

Forsberg F, Goldberg BB, Merritt CRB, Parker L, Maitino AJ, Palazzo JP, Needleman L. 2D and 3D contrast enhanced ultrasound for breast cancer detection. Submitted to *AIUM*, 2002.

Forsberg F, Kuruvilla B, Chaudhari MH, Yu A, Yoon R, Lee Y, Palzzo JP, Goldberg BB. Breast tumor neovascularity identified by contrast enhanced ultrasound and pathology. Submitted to *AIUM*, 2002.

June 29 - July 1, 1999. Ultrasonics International '99, Copenhagen, Denmark.

- Breast tumor vascularity identified by contrast enhanced ultrasound and pathology: initial results.

April 2 - 5, 2000 The 44th Annual Convention of the American Institute of Ultrasound in Medicine, San Francisco, CA, USA.

- Quantifying breast tumor neovascularity by contrast enhanced ultrasound and pathology: a comparative study.

June 8 – 11, 2000. Era of Hope, Dept. of Defense Breast Cancer Research Meeting, Atlanta, GA, USA.

- Contrast Enhanced Ultrasound Imaging of Breast Tumors.
- Contrast Enhanced Ultrasound Imaging of Breast Tumors (poster).

March 11 - 14, 2001 The 45th Annual Convention of the American Institute of Ultrasound in Medicine, Orlando, FL, USA.

- Contrast Enhanced Ultrasound and Mammography for Breast Cancer Detection.
- Does the Mechanical Index Predict Destruction Rates for Contrast Microbubbles ?

Degrees

A Master of Science degree in Biomedical Engineering was awarded from Drexel University to Manisha H. Chaudhari based in part on work performed as part of this grant. The PI (F. Forsberg) served as her supervisor.

A Bachelor of Science degree in Biomedical Engineering was awarded from Drexel University to Babita S Kuruvilla based in part on work performed as part of this grant. The PI (F. Forsberg) served as her supervisor.

Informatics

A study database has been designed and implemented in Filemaker Pro 5.0 (Filemaker Inc, Santa Clara, CA). This database contains all patient information (except names and other identifiers) and the results of the various ultrasound imaging modes as well as the pathology results.

8. CONCLUSIONS

In total, 55 patients with 16 cancers and 39 benign lesions have been enrolled in the study. These numbers were much less than anticipated, due to personnel illness and other protocol changes. Nonetheless, some significant results were obtained from this data set.

Standard 2D ultrasound achieved a sensitivity of 73 % and a specificity of 58 %, while 3D produced 75 % and 36 %, respectively. Contrast increased 3D sensitivity to 88 % and specificity to 47 %. The area under the ROC curve for the detection of breast cancer was 0.55 for 2D contrast, 0.60 for 3D ultrasound and 0.76 for 3D CAI with contrast ($p < 0.03$). Mammography produced an area of 0.86, which was significantly higher than that of all the ultrasound modalities ($p < 0.025$) except 3D ultrasound with contrast ($p = 0.16$). Furthermore, when mammography was combined with 2D contrast the area increased to 0.88, with 3D contrast to 0.89, and with all ultrasound modalities to 0.96 ($p < 0.001$). These results validate the fundamental hypothesis of this project; namely that the combination of 3D CAI and an ultrasound contrast agent increases the ability to diagnose breast cancer relative to current techniques.

The synergistic effect of combining 3D CAI with an ultrasound contrast agent was demonstrated, since the vascularity and the presence of anastamoses observed with contrast enhanced 3D were the only significant markers of malignancy found ($p < 0.02$). This indicates that the chaotic morphology of tumor neovascularity can indeed be evaluated with 3D contrast as hypothesized in the original grant application.

The histomorphometry system has been used to analyze vessel distribution and vessel density maps from 17 patients. Contrast enhanced color flow imaging was found to provide some quantitative parameters, which correlated with direct pathologic vascularity assessments such as the iMVD. Specifically, the microvessel area and count for vessels 30 to 39 μm in diameter were most significant. These results indicate that ultrasound imaging with contrast may produce

a quantitative measure of the neovascularity within breast tumors. However, the current patient population in the sub-study is small and further cases are currently being analyzed.

In summary, all tasks (1, 2 and 3) have been completed. The use of contrast enhanced 3D CAI for breast cancer diagnosis was shown to provide statistically significant improvements; albeit based on a smaller patient population than originally envisaged.

9. REFERENCES

1. Feig SA: Breast masses: Mammographic and sonographic evaluation. *Radiologic Clin North Am* 30:67-92, 1992.
2. Jackson VP: The Role of US in Breast Imaging. *Radiology*, 177:305-311, 1990.
3. Bohm-Velez M, Mendelson EB: Computed tomography, duplex Doppler ultrasound and magnetic resonance imaging in evaluating the breast. *Semin Ultrasound CT MR*, 10:171-176, 1989
4. Adler DD, Carson PL,. Rubin JM, Quinn-Reid D: Doppler ultrasound color flow imaging in the study of breast cancer: preliminary findings. *Ultrasound Med. Biol.*, 16: 553-559, 1990.
5. Weidner N, Folkman J, Pozza F, et al. Tumor angiogenesis: a new significant and independent prognostic indicator in early-stage breast cancer. *J Natl. Cancer Inst.*, 84: 1875-1887, 1992.
6. Goldberg BB. *Ultrasound contrast agents*. Martin Dunitz Ltd., London, UK, 1997.
7. Forsberg F, Merton DA, Liu JB, Needleman L, Goldberg BB: Clinical applications of ultrasound contrast agents. *Ultrasonics*, 36: 695 - 701, 1998.
8. Meyerowitz CB, Fleischer AC, Pickens DR, et al. Quantification of tumor vascularity and flow with amplitude color Doppler sonography in an experimental model: preliminary results. *J Ultrasound Med.* 15:827-, 1996.
9. Goldberg BB, Merritt CRB, Needleman L, Piccoli CW, Forsberg F, Parker L, Maitino A, Merton DA, Schultz SM, Rawool NM. Contrast Enhanced Ultrasound and Mammography for Breast Cancer Detection. *J Ultrasound Med*, 20: S95, 2001.
10. Barbareschi M, Weidner N, et al. Microvessel density quantification in breast carcinomas. *Appl. Immunohistochem.* 3:75-, 1995.
11. Bell D, Bamber J, Eckersley R. Segmentation and analysis of color Doppler images of tumor vasculature. *Ultrasound Med. Biol.* 21:635 -, 1995.
12. Burns P, Powers J, Simpson D, Brezina A, Kolin A, Chin C, Uhlendorf V, Fritzch T. Harmonic power mode Doppler using microbubble contrast agents: an improved method for small vessel flow imaging. *Proc IEEE Ultrason. Symp*, 1547-1550, 1994.
13. Esserman L, Hylton N, George T, Weidner N. Contrast-enhanced magnetic resonance imaging to assess tumor histopathology and angiogenesis in breast carcinoma. *The Breast J.* 5:13-21, 1999
14. Forsberg F, Chaudhari MH, Voodarla A, Goonewardene S, Needleman L, Goldberg BB: Qunatifying breast tumor neovascularity by contrast enhanced ultrasound and pathology: a comparative study. *J Ultrasound Med*, 19, S56 – S57, 2000.
15. Forsberg F, Chaudhari MH, Merritt CRB, Needleman L, Maitino AJ, Voodarla A, Goonewardene S, Goldberg BB. Contrast enhanced ultrasound imaging of breast tumors. *Proc Era of Hope, DoD Breast Cancer Research Meet*, 257 – 258, 2000.
16. Chaudhari MH, Forsberg F, Voodarla A, Saikali FN, Goonewardene S, Needleman L, Shi WT, Finkel GC, Goldberg BB: Breast tumor vascularity identified by contrast enhanced ultrasound and pathology: initial results. *Ultrasonics*, 38,105-109, 2000.
17. Forsberg F, Rawool NM, Merton DA, Liu JB, Goldberg BB: Contrast enhanced vascular 3D ultrasound imaging. Accepted for publication in *Ultrasonics,* 2002.

18. Forsberg F, Goldberg BB, Merritt CRB, Parker L, Maitino AJ, Palazzo JP, Needleman L. 2D and 3D contrast enhanced ultrasound for breast cancer detection. Submitted to *AIUM*, 2002.
19. Forsberg F, Kuruvilla B, Chaudhari MH, Yu A, Yoon R, Lee Y, Palzzo JP, Goldberg BB. Breast tumor neovascularity identified by contrast enhanced ultrasound and pathology. Submitted to *AIUM*, 2002.

10. TABLES

Table 1. Mean patient age and maximum lesion diameter (± one standard deviation) for benign and malignant cases. There were no statistical differences between the two groups.

	age [years]	size [mm]
benign	51 ± 11	15 ± 9
malignant	56 ± 8	10 ± 5

Table 2. Sensitivity and specificity of the six imaging modalities. There were no statistically significant differences in specificity. The sensitivity of mammography exceeded all ultrasound modalities ($p < 0.01$). The sensitivity of 3D ultrasound was significantly higher than 2D ultrasound ($p = 0.046$), while 3D with contrast did better than both ($p = 0.008$ & $p = 0.018$, respectively) and better than grayscale ultrasound ($p = 0.039$).

	grayscale	2D CAI baseline	2D contrast	3D CAI baseline	3D contrast	mammo
sensitivity [%]	67	73	53	75	88	100
specificity [%]	63	58	39	36	47	41

Table 3. Area under the ROC (A_z) for the six imaging modalities individually. A_z was significantly higher for 3D contrast than for 2D with and without contrast and for 3D ultrasound without contrast ($p < 0.03$). Mammography produced an A_z, which was significantly higher than all ultrasound modalities ($p < 0.025$) except 3D ultrasound with contrast ($p = 0.16$). Somewhat surprisingly, the A_z of 2D ultrasound was significantly higher without than with contrast ($p = 0.026$).

	grayscale	2D CAI baseline	2D contrast	3D CAI baseline	3D contrast	mammo
A_z	0.65	0.66	0.55	0.60	0.76	0.86

Table 4. Area under the ROC (A_z) for the six imaging modalities combined. Mammography combined with all ultrasound modalities produced an A_z of 0.96, which was significantly higher than all other combinations ($p < 0.05$) with the exception of 3D baseline, which showed a trend towards significance ($p = 0.068$).

	mammo & grayscale	mammo & 2D CAI baseline	mammo & 2D contrast	mammo & 3D CAI baseline	mammo & 3D contrast	mammo & all US	all US
A_z	0.88	0.89	0.88	0.88	0.89	0.96	0.83

Table 5. Sensitivity and specificity for 2D and 3D ultrasound imaging with contrast split by agent. There were no statistically significant differences in specificity. The sensitivity of 3D with Optison was significantly higher than 3D with Levovist ($p = 0.007$).

	Levovist		Optison	
	2D contrast	3D contrast	2D contrast	3D contrast
sensitivity [%]	60	80	50	91
specificity [%]	50	60	32	38

Table 6. Procedure for image analysis of breast tumor slides(steps not used in the Barbareschi method are marked with asterisks).

1) *Optional histogram map applied to original image if CD31 staining very poor
2) *Open and Sharpen filters are used on the original image
3) Saturation and Blue images are extracted from the original image in RGB and HSI color models. In the Blue image, the brown stain appears the darkest and in the Saturation image, the brown stain appears lightest.
4) Subtraction of Blue image from the Saturation image resulting in an image in which only pixels corresponding to the brown stain of the original image are present. Theoretically automatic detection of the microvessels is possible by selecting all pixels greater than a gray value of 1.
5) Manual segmentation of the gray level pixels corresponding to the brown stain
6) Automated counting and measuring microvessels and exporting the raw data to Microsoft Excel

Table 7. Linear regression r^2 values with (p) if significant.

Data sets	Pathologic parameters	EXPANDED DATA Ultrasonic % Color Pixels		REDUCED DATA Ultrasonic % Color Pixels	
		Pre injection	Post injection	Pre injection	Post injection
All masses	Total MVA	0	0	0	0
$n_e = 83$	Total MVC	0	0	0	0
$n_r = 52$	MVA-5 ranges	0.05	0.27 (.0002)	0.13	0.22 (.04)
	iMVD-5 ranges	0.01	0.20 (.003)	0.04	0.48 (<.0001)
Benign	Total MVA	0	0	0	0
	Total MVC	0	0	0	0
$n_e = 53$	MVA-5 ranges	0.10	0.47 (<.0001)	0.34 (.032)	0.42 (.01)
$n_r = 34$	iMVD-5 ranges	0.01	0.18	0.01	0.63 (<.0001)
Malignant	Total MVA	0	0	0	0
	Total MVC	0	0	0	0
$n_e = 30$	MVA-5 ranges	0.47 (.006)	0.47 (.007)	0.75 (.002)	0.62 (0.025)
$n_r = 18$	iMVD-5 ranges	0.48 (.005)	0.44 (.01)	0.58 (.04)	0.47

Table 8. T-statistic for significant variables: expanded data and % color pixels (p value). Notice that the malignant iMVD post injection correlation was only significant collectively.

Data set	Pathologic parameters	T – statistic value
All masses (post inj)	MVA by 30-39 μm Vessels	4.75 (<.0001)
	MVA by 20-29 μm Vessels	2.60 (.006)
All masses (post inj)	IMVD in 30-39 μm Range	4.10 (<.0001)
	IMVD in 50 & up μm Range	2.76 (.004)
	IMVD in 20-29 μm Range	1.66 (.05)
Benign (post inj)	MVA by 30-39 μm Vessels	5.79 (<.0001)
	MVA by 20-29 μm Vessels	2.06 (.02)
Malignant (post inj)	MVA by 40-49 μm Vessels	3.77 (.0005)
Malignant (pre inj)	MVA by 40-49 μm Vessels	3.36 (.001)
Malignant (pre inj)	IMVD in 30-39 μm Range	2.35 (.014)
	IMVD in 40-49 μm Range	2.34 (.014)
	IMVD in 10-19 μm Range	2.26 (.017)
	IMVD in 20-29 μm Range	2.24 (.017)
	IMVD in 50 & up μm Range	2.13 (.017)

Table 9. T-statistic for significant variables: reduced data and % color pixels (p value). Notice that the benign MVA pre injection correlation was only significant collectively.

Data Set	Pathologic Parameters	T – statistic Value
All masses (post inj)	MVA by 30-39 μm Vessels	3.05 (.002)
	MVA by 20-29 μm Vessels	2.30 (.01)
All masses (post inj)	iMVD in 30-39 μm Range	5.21 (<.0001)
	iMVD in 40-49 μm Range	5.07 (<.0001)
	iMVD in 10-19 μm Range	4.96 (<.0001)
	iMVD in 20-29 μm Range	4.89 (<.0001)
	iMVD in 50 & up μm Range	4.72 (<.0001)
Benign (post inj)	MVA by 30-39 μm Vessels	4.05 (.0002)
	MVA by 20-29 μm Vessels	2.69 (.006)
Benign (post inj)	iMVD in 30-39 μm Range	6.16 (<.0001)
	iMVD in 40-49 μm Range	5.98 (<.0001)
	iMVD in 10-19 μm Range	5.93 (<.0001)
	iMVD in 20-29 μm Range	5.87 (<.0001)
	iMVD in 50 & up μm Range	5.74 (<.0001)
Malignant (post inj)	MVA by 40-49 μm Vessels	3.69 (.002)
Malignant (pre inj)	MVA by 40-49 μm Vessels	4.95 (.0002)
Malignant (pre inj)	iMVD in 40-49 μm Range	2.11 (.028)
	iMVD in 30-39 μm Range	2.10 (.029)
	iMVD in 10-19 μm Range	2.02 (.033)
	iMVD in 20-29 μm Range	1.99 (.035)
	iMVD in 50 & up μm Range	1.89 (.041)

11. FIGURES

Figure 1. Example of infiltrating and intraductal breast cancer (arrows) imaged in 2D CAI mode pre (A) and post (B) injection of 1.0 ml of Optison.

Figure 2. Example of ductal cancer in situ (arrows) imaged in 3D CAI mode pre (A) and post (B) injection of 1.0 ml of Optison.

Figure 3. Individual ROC curves for the six imaging modalities (line symbols: grayscale -x-, 2D CAI -.-, 2D contrast -o-, 3D CAI - □-, 3D contrast -◊- and mammography -Δ-).

Figure 4. ROC curves for mammography (dashed line), mammography combined with grayscale ultrasound (dash dot line), with contrast enhanced 3D CAI (dotted line), and with all five ultrasound imaging modes (solid line).

(A)

(B)

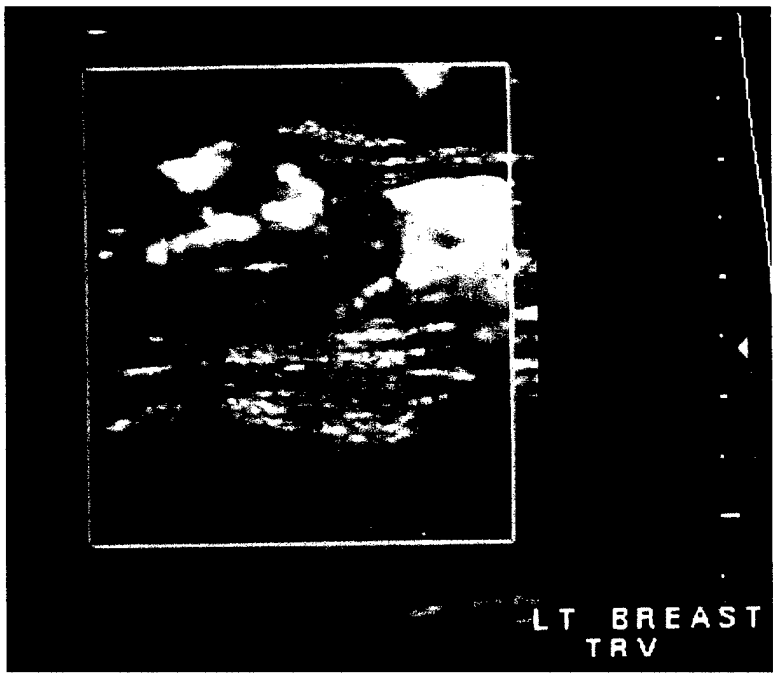

Figure 1. Example of infiltrating and intraductal breast cancer (arrows) imaged in 2D CAI mode pre (A) and post (B) injection of 1.0 ml of Optison.

(A)

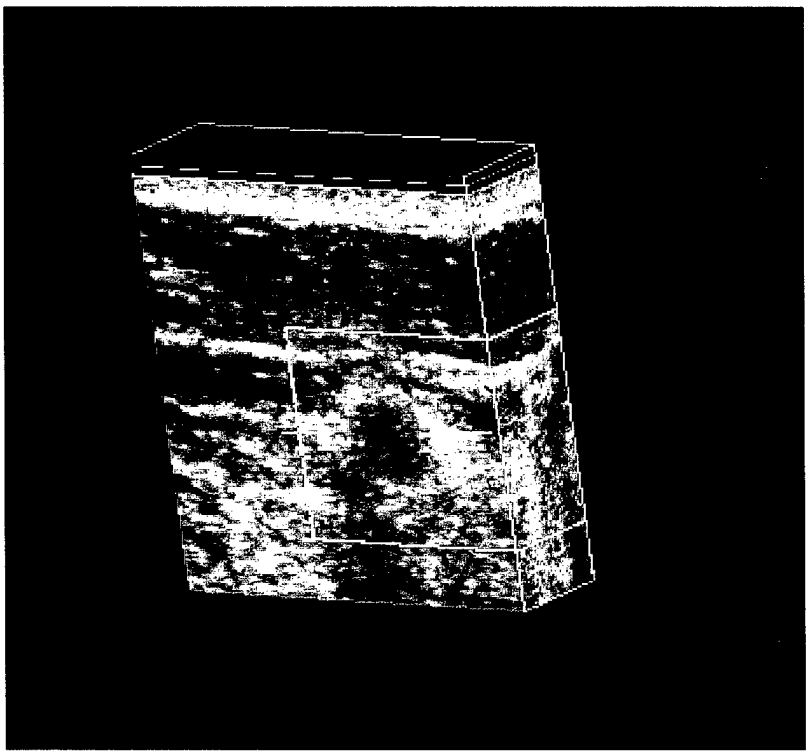

(B)

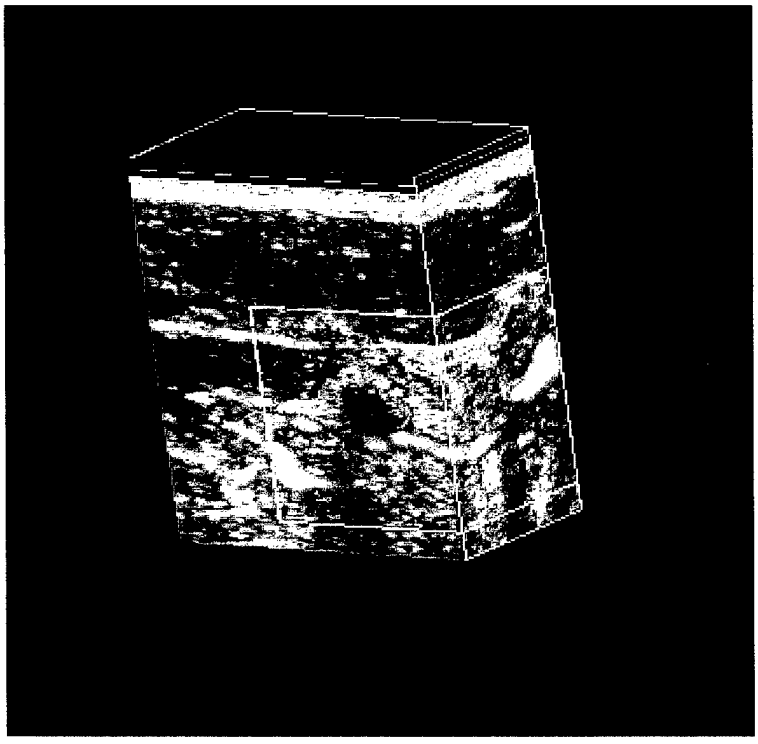

Figure 2. Example of ductal cancer in situ (arrows) imaged in 3D CAI mode pre (A) and post (B) injection of 1.0 ml of Optison.

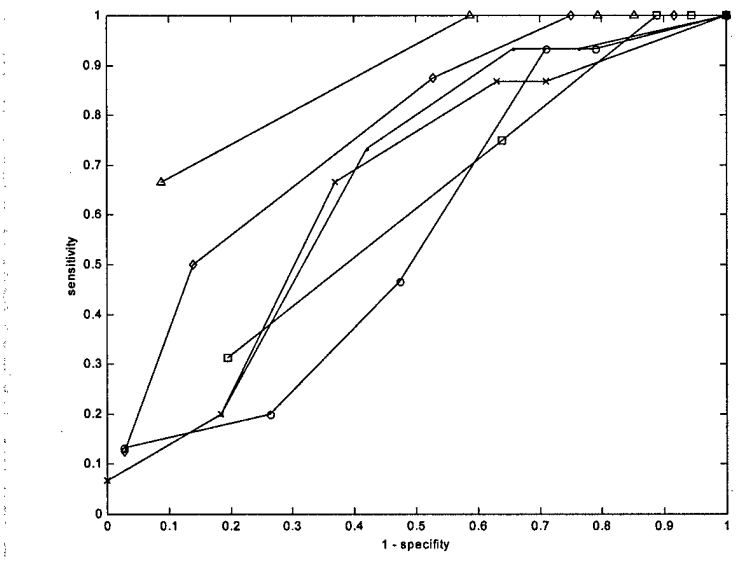

Figure 3. Individual ROC curves for the six imaging modalities (line symbols: grayscale -x-, 2D CAI -.-, 2D contrast -o-, 3D CAI - □-, 3D contrast -◊- and mammography -Δ-).

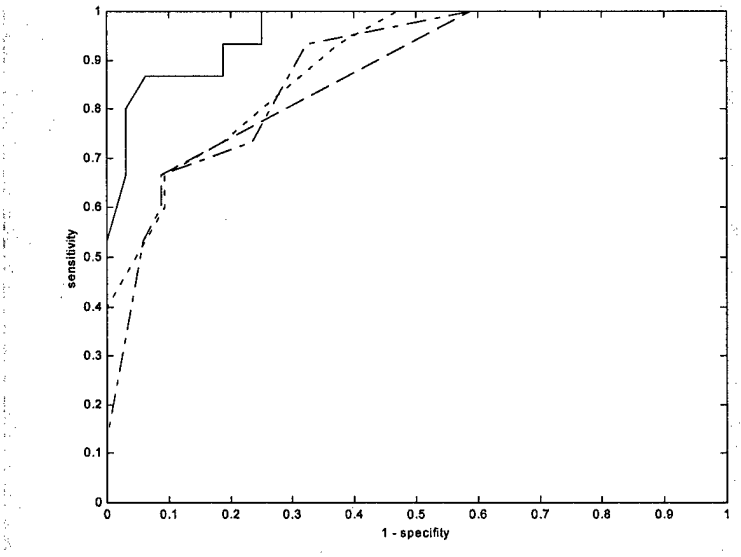

Figure 4. ROC curves for mammography (dashed line), mammography combined with grayscale ultrasound (dash dot line), with contrast enhanced 3D CAI (dotted line), and with all five ultrasound imaging modes (solid line).

Appendix I

The Statement of Work from the original proposal:

Technical objectives 2 - 3
Task 1: Software development (months 1 - 6)

a. Develop image analysis software for the histomorphometry system to allow vessel distribution (i.e., histogram) and vessel density maps to be produced from 3D image data.

b. Develop 3D parameter extraction algorithms for the LIS 6000A system e.g., counting the number of interconnecting branches ("AV-shunts") and scoring the vessel tortuousity in collaboration with the consultant. Depending on the outcome of the statistical analysis, it is conceivable that new parameters will have to be extracted at a later date. Since the acquired 3D data volumes can be processed repeatedly this does not impact on the study design, it only demonstrates the flexibility of the data.

Technical objective 1
Task 2: Data collection (months 1 - 36)

a. recruit 50 patients per year. This is about half of the anticipated number of patients being enrolled in the NIH supported contrast study.

b. perform 3D CAI contrast studies as part of the already funded NIH project. This involves an extra injection of contrast (within the permitted total dose) and will add no more than 20 minutes to the total duration of the contrast study.

c. research coordinator to collect clinical information (pathology results, etc.).

Technical objectives 2 - 3
Task 3: Data analysis (months 6 - 36)

a. incorporate 3D imaging findings into the existing database (developed for the NIH supported contrast study).

b. quantitate 3D CAI results in collaboration with the consultant.

c. perform ROC analysis in collaboration with the statistician.

d. perform remaining statistical analysis in collaboration with the statistician.

Appendix II

Reprint of article which will appeared in *Ultrasonics*, 2002.

Contrast Enhanced Vascular 3D Ultrasound Imaging

F. Forsberg, N. M. Rawool, D. A. Merton, J. B. Liu, B. B. Goldberg.

Department of Radiology, Thomas Jefferson University, Philadelphia, PA 19107, USA.

Abstract: In other imaging modalities three dimensional (3D) data displays are well established; not so in ultrasound. Due to the real-time requirements of ultrasound the time available to compute 3D displays is limited, particularly when flow data is acquired with Doppler techniques. Consequently, it is only recently that improvements in computer processing power have resulted in useful vascular 3D ultrasound scans. Many manufacturers have now implemented free-hand 3D power Doppler capabilities on their scanners. However, to obtain flow signals from smaller vessels associated e.g., with tumor neovascularity, may very well require the introduction of a microbubble based ultrasound contrast agent into the blood stream. Given the up to 30 dB enhancement of Doppler signals produced by the contrast microbubbles quite spectacular vascular 3D images are feasible. Moreover, new contrast imaging techniques, such as harmonic imaging, have now permitted 3D vascular information to be acquired and displayed in gray-scale with the associated improvement in resolution. In this paper we will review different aspects of contrast enhanced vascular 3D ultrasound imaging including implementation, contrast specific techniques and in vivo imaging.

Keywords: 3D ultrasound imaging, contrast agents, 3D pulse inversion harmonic imaging.

Correspondence to: Flemming Forsberg, Ph.D.
Department of Radiology, Suite 763J, Main Building, Thomas Jefferson University
132 South 10th Street, Philadelphia, PA 19107, USA
Fax +1 - 215 - 955 8549; email: forsberg@esther.rad.tju.edu

1. Introduction

In other imaging modalities, such as computed tomography (CT) and magnetic resonance imaging (MRI), three dimensional (3D) data displays are well established and increasingly used in the diagnostic decision making; not so in ultrasound. Due to the real-time (or at least near real-time) requirements of ultrasound imaging the time available for acquisition and processing of a 3D volume of data is very limited. This is particularly true, when blood flow data is acquired with Doppler ultrasound using multiple firing techniques. Consequently, it is only in the last few years that improvements in computer processing power and visualization techniques have resulted in reports on the clinical use of vascular 3D ultrasound scanning [1-4].

The clinical applications of vascular 3D ultrasound imaging include among others the assessment of flow in the kidney, placenta, prostate and carotid artery [1, 3]. The benefit is being able to localize a functional abnormality relative to the underlying anatomy. One major advantage in vascular 3D imaging is the relative ease involved in segmenting flow data from tissue echoes. Blood flow signals, whether from various color flow modes or simple signal voids (i.e., black vessels seen in grayscale), are straightforward to separate due to the clear interfaces present. Inverse minimum projection has been used successfully to display larger vessels within a gray-scale tissue volume [3]. However, to obtain flow signals from smaller vessels e.g., associated with tumor neovascularity, may very well require the introduction of a microbubble based ultrasound contrast agent into the blood stream to increase signal-to-noise-ratios [5].

3D Data Acquisition

Producing an accurate 3D ultrasound image relies critically on the data acquisition technique, and on exact definition of the 3D volume. In a static image collection modality with fixed slice thickness, such as CT or MRI, the geometry of the 3D volume is given, but in

ultrasound a different approach has to be taken. The simplest way of accurately defining the 3D volume is to mount a conventional transducer in a mechanical arm and move the probe under automatic control. This approach is often limited to movement along a single axis and can be difficult to carry out on curved surfaces such as the breast. An alternative is to use a dedicated 3D transducer, comprising of a conventional transducer mounted with a stepping motor in a hand held assembly (internal or external to the probe housing). The motor either translates or rotates the transducer around an axis, which defines the 3D volume.

The 3D volume can also be specified by placing sensors on a conventional transducer and then tracking its location in space via remote localizers. Acoustic, optical and magnetic positioning devices have been utilized e.g., [6-7]. Even though these approaches offer great flexibility of movement, they require additional sensor equipment to be placed near the patient (e.g., microphones or a magnetic field generator) and also lack sufficient accuracy to be clinically useful. A more elegant approach is afforded by 2D electronic arrays, which permit focussing in the elevation plane as well as true angle-independent flow measurements [8]. Commercial 2D arrays are emerging and probably represent the ultimate technique for real-time 3D ultrasound data acquisition.

For current vascular 3D ultrasound imaging, most manufacturers have relied on complete free-hand acquisition of power Doppler data due to the relative ease of implementation. The assumption is that the sonographer scans at a constant rate and in a clean sweep. However this, obviously, limits geometric accuracy. This technique relies on correlation analysis of speckle patterns and image features from slice to slice to reconstruct the 3D volume.

2. Vascular 3D Ultrasound Imaging

The ability of ultrasound to perform real-time studies of blood flow is clinically very

important. Thus, it is not surprising that the prospect of combining color flow imaging with 3D displays has aroused interest; in spite of the considerable demands on computer resources. The clinical applications of vascular 3D ultrasound imaging include the visualization of cardiac jets due to valve defects and the assessment of carotid stenoses, which can be difficult to do using conventional ultrasound. Vascular 3D imaging has also been attempted in the kidney, placenta and prostate to monitor tumor flow after radiation therapy as well as in the brain to overcome the difficulties of transcranial Doppler to globally evaluate the major cerebral arteries [3]. The benefit of 3D ultrasound is being able to localize a functional abnormality relative to the underlying anatomy.

Despite the invasive nature of intravascular ultrasound imaging, encouraging results have been reported, including vascular 3D imaging of the coronary arteries [9]. The much higher imaging frequencies used (20 – 40 MHz) provide superior resolution, while the corresponding loss in penetration is immaterial to intravascularly positioned catheters.

One way to increase the quality of the 3D display is to acquire power Doppler instead of color Doppler images. Power Doppler has the ability to display flow in smaller vessels as well as showing vessels over a longer length than has conventional color Doppler. This increase in display dynamic range is achieved by sacrificing directional and velocity information, which makes vessels in power Doppler appear more like those of x-ray angiograms. The added completeness of the depiction of the vasculature also results in more complete 3D flow images. Most manufacturers have now implemented free-hand 3D power Doppler capabilities on their scanners. Nonetheless the ability of ultrasound flow imaging to detect and display vessels less than 300 μm in diameter is still limited.

3. Vascular 3D Ultrasound Imaging with Contrast

Ultrasound imaging has become a very successful modality in clinical radiology and cardiology, because of its ability to provide non-invasive, 2D and 3D images of soft tissue structures and blood flow without ionizing radiation. Nonetheless, conventional Doppler ultrasound has limited ability to detect blood flow in small vessels or in deep tissue owing to poor reflectivity of blood and strong echoes from stationary tissues. Moreover, it is not always possible to achieve sufficient contrast resolution in grayscale imaging to differentiate between normal and diseased tissues.

Ultrasound Contrast Agents

Alleviating the above mentioned limitations form the rationale behind the rapid development of contrast agents for ultrasound; a variety of which are currently commercially available or under development [5, 10]. Ultrasound contrast agents consist of gas-filled microbubbles 1 to 8 μm in diameter. Most contrast agents are stabilized against dissolution and against coalescence by the presence of additional materials at the gas-liquid interface. In some cases, this material is an elastic solid shell, which enhances stability by supporting a strain to counter the effect of surface tension. In other cases, the material is one or a combination of two or more surfactants, which promote stability by greatly reducing the surface tension at the interface. Most of the newer vascular ultrasound contrast agents are composed of perfluorocarbon-filled microbubbles (due to the low solubility in blood) which produce more than 5 minutes of enhancement.

Contrast agents promise to improve the sensitivity and specificity of diagnostic 2D and 3D ultrasound imaging by increasing blood flow signal intensities and, thus, signal-to-noise ratios by up to 30 dB. Some agents also improve gray-scale visualization of the flowing blood to such a degree that the tissue echogenicity increases (parenchymal enhancement). Microbubbles

within the small vessels of an organ can, thus, provide an indication (albeit qualitatively) of perfusion.

Clinical Applications

Intravenous vascular contrast agents will undoubtedly be used extensively to diagnose vascular disease (e.g., stenoses and areas of ischemia) as well as tumors. The combination of contrast agents and 3D imaging should produce a further increase in diagnostic confidence. A variety of tumors have been evaluated in humans including in the liver, kidney, ovary, pancreas, prostate and breast [5]. In these studies, enhancement of both color and spectral Doppler flow signals from intra-tumoral blood vessels was achieved. This is a significant result since one of the early changes that differentiate normal from cancerous tissues is the process by which the tumor develops its blood supply i.e., tumor angiogenesis, which can be an independent marker of malignancy [11].

We have developed a unique new animal model for investigating prostate cancer and 3D ultrasound imaging [12]. A Canine Transmissible Venereal Sarcoma (CTVS) cell line (50 million cells/ml) was injected directly into canine prostates. This cell line is capable of growing and producing a cancer-like mass in the dog prostate, and 20-30 days post injection, multi-nodular tumors were evident in the prostate. Transrectal power Doppler of the prostate was performed in 3D with a C9-5 end-fire probe and an HDI 3000 scanner (ATL, Bothell, WA). The 3D imaging technique used in this case is based on free hand data acquisition and reconstruction of power Doppler images stored in the scanner's cine-loop.

An example of the minimal vascularity seen within a normal canine prostate pre contrast is given in Figure 1A. Post injection of contrast a marked increase in vessel visualization occurs and a distinct spoke-like flow pattern is seen with 3D imaging (Fig. 1B). With contrast enhanced

3D imaging a marked difference can be seen between normal prostatic vascularity and the disturbed flow patterns caused by a CTVS tumor (Fig. 1C).

As part of a Department of Defense (USAMRMC) funded effort to investigate contrast enhanced 2D and 3D breast tumor imaging, patients with solid breast masses received Optison® (dosage: 1 ml; Mallinckrodt, St. Louis, MO). Pre and post contrast power Doppler images of the masses were obtained using an HDI 3000 unit. In this study, the 3D data acquisition post-processing and reconstructions were performed with an LIS 6000A system (Life Imaging Systems Inc, London, Canada), which utilizes a conventional transducer mounted in an external assembly controlled by a stepping motor. The 3D power Doppler data sets were reconstructed, with no loss of registration accuracy (unlike the previous example) providing both multi-perspective maximum-intensity-projection visualization and 2D planar views.

Figure 2 demonstrates the ability of 3D ultrasound imaging to depict human breast tumor neovascularity. An in-situ and invasive breast carcinoma appears almost completely avascular before contrast administration. After injection of Optison, peripheral as well as central tumor neovascularity is clearly seen (Fig. 2B). Moreover, several larger feeding vessels around the tumor are visualized in 3D demonstrating their spatial relationships, which make up the complex angiogenic vascular architecture associated with this malignant tumor. Initial receiver operating characteristics (ROC) analysis of 55 patients found that 3D ultrasound with contrast significantly improved the diagnosis of breast cancer compared to 3D without contrast and 2D with contrast (area under the curve increased from 0.60 and 0.51 to 0.76; $p < 0.01$).

Visualization of the vasculature might be further enhanced with the use of harmonic imaging (HI), which represents yet another advance in ultrasound imaging of contrast agents [13-15]. HI utilizes the ability of microbubbles to oscillate nonlinearly in the ultrasound field. The microbubbles act as harmonic oscillators producing echo signals with significant energy

components at the resonance (or fundamental) frequency as well as at its higher and lower harmonics. HI preferentially enhances and displays contrast signals rather than surrounding tissue echoes by transmitting at the fundamental transducer frequency (f_o) and receiving at the second harmonic ($2f_o$). Since ordinary tissue predominantly reflects ultrasound at the frequency of insonation, most harmonic signals will come from contrast material. Hence, the contrast-to-tissue signal-to-noise ratio improves markedly [5].

Further improvements are possible with the use of pulse inversion HI [16-18]. This technique cancels first harmonic (linearly scattered) signals by transmitting a pulse sequence where each pulse is an inverted copy of the previous pulse, and then summing the echoes from subsequent pulses (resulting in zero under linear scattering conditions). Hence, echoes from stationary tissue will be suppressed. However, nonlinear echoes associated with contrast microbubbles will not cancel out and, thus, can be preferentially detected and displayed. This potentially makes "microbubble only" imaging i.e., an "ultrasound arteriogram" feasible as demonstrated in Figure 3. Here a rabbit kidney is shown imaged in 3D pulse inversion HI mode. The blood flow in the renal hilum as well as in larger and smaller segmental renal arteries can clearly be seen following administration of Sonazoid® (Nycomed-Amersham, Oslo, Norway). Pulse inversion harmonic imaging has the potential to show not only normally perfused organs but also, more clinically important, perfusion abnormalities.

The importance of rapidly diagnosing and treating patients presenting with active bleeding due to trauma has long been recognized as an important clinical goal [19]. We have used transabdominal gray scale pulse inversion HI was to assess active bleeding sites within the abdominal organs of a mongrel dog [20]. An internal bleeding model was created by inserting an 18-gauge biopsy needle percutaneously into the parenchyma of the spleen under ultrasound guidance. A laceration was made by the needle within this organ. Sonazoid was injected

intravenously (dose: 0.01µl/kg) so that contrast was circulating within the animal's blood stream prior to creating the bleeding site. Three-dimensional gray scale pulse inversion HI of the spleen was then performed (Fig. 4), resulting in the detection of the active bleeding site within the parenchyma. Thus, contrast enhanced 3D imaging may provide valuable information about spatial relationships and pathology related to active bleeding sites.

4. Conclusions

Three-dimensional grayscale ultrasound imaging has already become a clinical reality in obstetrics (in other specialties clinical acceptance is lacking behind, mainly due to image quality concerns). Now with the advent of ultrasound contrast agents, it appears that contrast enhanced vascular 3D imaging is poised to mature into a clinically useful, radiological imaging modality. This will expand the diagnostic capabilities of vascular ultrasound imaging to improve the detection of flow in smaller and deeper vessels throughout the body. It should enhance the assessment of organ vascularity as well as the detection and differential diagnosis of tumors and other areas with abnormal vascularity. The speed at which this will occur, obviously depends highly on the approval of suitable ultrasound contrast agents by the Food and Drug Administration.

Future improvements in 3D imaging equipment (in particular faster acquisition and processing capabilities), combined with the wide variety of new ultrasound contrast agents being developed, will make contrast enhanced 3D ultrasound imaging an even more powerful diagnostic tool.

Acknowledgment

This work was supported in part by DAMD17-97-1-7116, Mallinckrodt, St. Louis, MO,

USA and Nycomed-Amersham, Oslo, Norway.

References

[1] A. Fenster, D.B. Downey, 3-D ultrasound imaging: a review, IEEE Eng Med Biol Mag 15 (1996) 41.

[2] C.J. Ritchie, W.S. Edwards, L.A. Mack, D.C. Cyr, Y. Kim, Three-dimensional ultrasonic angiography using power mode Doppler, Ultrasound Med Biol 22 (1996) 277.

[3] T.R. Nelson, D.H. Pretorius, Three-dimensional ultrasound imaging, Ultrasound Med Biol 24 (1998) 1243.

[4] R. Campani, O. Bottinelli, F. Calliada, D. Coscia, The latest in ultrasound: three-dimensional imaging. Part II, Eur J Radiol 22 (1996) 277.

[5] B.B. Goldberg, J.S. Raichlen, F. Forsberg, Ultrasound Contrast Agents: Basic Principles and Clinical Applications, 2nd Ed, Martin Dunitz Ltd., London, 2001.

[6] P.A. Picot, D.W. Rickey, R. Mitchell, R.N. Rankin, A. Fenster, Three-dimensional colour Doppler imaging, Ultrasound Med Biol 19 (1993) 95.

[7] O.H. Gilja, T. Hausken, S. Olafsson, K. Matre, S. Ødegaard, In vitro evaluation of three-dimensional ultrasonography based on magnetic scanhead tracking, Ultrasound Med Biol 24 (1998) 1161.

[8] E.D. Light, R.E. Davidsen, J.O. Fiering, T.A. Hruschka, S.W. Smith, Progress in 2-D arrays for real time volumetric imaging, Ultrasonic Imaging 20 (1998) 235.

[9] J.B. Liu, S. Miller, D. Bagley, J. Bonn, F. Forsberg, Endoluminal 3D ultrasound, In: Endoluminal Ultrasound: Vascular and Nonvascular Applications, JB Liu & BB Goldberg (eds.), Martin Dunitz Ltd., London, (1998) 325.

[10] F. Forsberg, D.A. Merton, J.B. Liu, L. Needleman, B.B. Goldberg, Clinical applications of

ultrasound contrast agents, Ultrasonics 36 (1998) 695.

[11] J. Folkman, What is the evidence that tumors are angiogenesis dependent? J Natl Cancer Inst 82 (1990) 4.

[12] F. Forsberg, M.T. Ismail, E.K. Hagen et al. Ultrasound contrast imaging of prostate tumors. In: Acoustical Imaging Vol. 24, H Lee (ed.), Plenum Press, New York, (2000) 309.

[13] B.A. Schrope, V.L. Newhouse, V. Uhlendorf, Simulated capillary blood flow measurement using a nonlinear ultrasonic contrast agent, Ultrasonic Imaging 14 (1992) 134.

[14] N. de Jong, R. Cornet, C.T. Lance, Higher harmonics of vibrating gas-filled microspheres. Part one: simulations, Ultrasonics 32 (1994) 447.

[15] N. de Jong, R. Cornet, C.T. Lance, Higher harmonics of vibrating gas-filled microspheres. Part two: measurements. Ultrasonics 32 (1994) 455.

[16] D.H. Simpson, C.T. Chin, P.N. Burns, Pulse inversion Doppler: a new method for detecting nonlinear echoes from microbubble contrast agents, IEEE Trans Ultrason Ferroelec Freq Contr 46 (1999) 372.

[17] T. Albrecht, C.W. Hoffman, S. Schettler, et al. B-mode enhancement using phase-inversion US with air-based microbubble contrast agent: initial experience in humans, Radiology 216 (2000) 273.

[18] F. Forsberg, J.B. Liu, H.J. Chiou, N.M. Rawool, L. Parker, B.B. Goldberg, Comparison of fundamental and wideband harmonic contrast imaging of liver tumors Ultrasonics 38 (2000) 110.

[19] H.L. Pachter, A.A. Guth, S.R. Hofstetter, Changing patterns in the management of splenic trauma: the impact of nonoperative management, Ann Surg 227 (1998) 98.

[20] J.B. Liu, D.A. Merton, B.B. Goldberg, N.M. Rawool, F. Forsberg, Contrast-enhanced 2-D and 3-D sonography for detection of intra-abdominal hemorrhage, Submitted to J Ultrasound Med (2001).

Captions

Figure 1 3D power Doppler imaging of a canine prostate. (A): pre contrast the vascularity visualized within the gland is minimal; (B): post injection a marked increase in vessel visualization occurs and a distinct spoke-like flow pattern is seen. (C): Disrupted prostatic flow patterns, due to a CTVS tumor (T), seen post contrast injection.

Figure 2 3D power Doppler imaging of patient with an in situ and invasive breast carcinoma. (A): pre contrast the tumor (arrows) appears avascular with only two, small vessels seen in the surrounding parenchyma; (B): post injection of Optison a marked increase in vascularity is seen (both within the tumor and in the surrounding tissue) increasing the delineation of the tumor.

Figure 3 Gray-scale 3D pulse inversion harmonic imaging of a rabbit kidney (arrow heads) following administration of Sonazoid. This display is referred to as a "3D ultrasound arteriogram." Notice the small segmental renal arteries depicted (arrows) as well as the perfusion blush of the renal cortex.

Figure 4 Gray-scale 3D pulse inversion harmonic imaging of contrast filled blood pooling from an active bleeding site (arrows) within a canine spleen. Note the fine detail of the normal splenic vasculature.